Open Access



Asian Journal of Environmental Research
E-ISSN: 3047-4930
DOI: https://doi.org/10.69930/ajer.v3i3.981
Research Article

ScienceTech Group

Vol. 3 (3), 2026
Page: 338-351

Forest-Fire Susceptibility Mapping Using Bioclimatic Predictors and MaxEnt: A Case Study of Ureng and Asilulu, Ambon Island

Rizky Ahmad Laitupa [1,*], Ahmad Rifai [2], Halim [3], Heinrich Rakuasa [4,]**

[1] Department of Regional and Rural Development Planning, IPB University, Indonesia
[2] Department of Environmental Science, Graduate School of Sustainable Development, Universitas Indonesia, Indonesia
[3] Department of Coastal and Marine Resources Management, IPB University, Indonesia
[4] Department of Geoecology, National Research Tomsk State University, Russian Federation
*Email (corresponding author): rizkylaitupa10@gmail.com, heinrich.rakuasa@yandex.ru

Abstract. *Forest fires are an important environmental hazard in small-island ecosystems because seasonal climatic variability can influence vegetation moisture, fuel availability, and fire susceptibility. This study aimed to model and spatially assess forest fire vulnerability in Negeri Ureng and Negeri Asilulu, Ambon Island, Indonesia, using the Maximum Entropy (MaxEnt) approach based on bioclimatic variables. The analysis utilized 25 historical fire-occurrence locations derived from MODIS and VIIRS/FIRMS data and five bioclimatic predictors from WorldClim version 2.1 at approximately 1 km spatial resolution, including Annual Mean Temperature (BIO1), Isothermality (BIO3), Maximum Temperature of the Warmest Month (BIO5), Temperature Annual Range (BIO7), and precipitation-related variables. The model demonstrated excellent predictive performance, with an AUC value of 0.94 and close agreement between the test omission rate and predicted omission rate, indicating good model stability and generalization. Precipitation Seasonality (BIO15) was the most influential predictor, contributing 54.6% with a permutation importance of 55.4%, followed by Annual Mean Temperature (BIO1), contributing 24.7% with a permutation importance of 27.0%. Jackknife analysis further confirmed the dominant role of BIO15, as its removal produced the largest reduction in training gain. Spatially, 230.3964 km² (81.77%) of the study area was classified as Very Low and Low Risk, whereas 51.3945 km² (18.24%) was classified as High and Very High Risk. These findings indicate that seasonal precipitation variability and temperature conditions are key environmental controls of forest fire vulnerability. The resulting vulnerability map provides an important basis for prioritizing fire monitoring, early warning, and mitigation strategies, particularly in highly vulnerable areas during periods of increasing seasonal drought stress.*

Keywords: *Ambon; Bioclimatic; Forest Fire; MaxEnt*

1. Introduction

Forest and land fires have emerged as some of the most destructive environmental disasters of the Anthropocene. Their frequency and intensity have increased significantly due to the global climate change crisis and interannual climate variability (1). Globally, the escalation of fire events not only damages ecosystem structure and function and reduces biodiversity, but also triggers massive carbon emissions that accelerate global warming (2), (3). Extreme climate phenomena, such as the El Niño–Southern Oscillation (ENSO), induce prolonged dry periods and rising surface temperatures, directly reducing fuel moisture content and creating highly vulnerable microclimatic conditions for the spread of fire hotspots

Received: 6 October 2026 / Accepted: 9 November 2026 / Available online:19 November 2026

(2). These adverse impacts also contribute to public health crises caused by exposure to transboundary smoke pollution, as well as massive socioeconomic losses in various parts of the world (4).

As the country with the third-largest tropical forest area in the world, Indonesia is highly vulnerable to forest and land fires (5,6). Recurrent severe fires, particularly during the 2015, 2019, and 2023 ENSO events, burned millions of hectares of forests and peatlands in Sumatra, Kalimantan, and Papua (5). The primary drivers of fires in Indonesia result from the complex interaction between meteorological factors, particularly extreme drought, and dominant anthropogenic pressures. These pressures include slash-and-burn agricultural practices, plantation land clearing, and vegetation-cover conversion (7). The impacts of these fires not only generate billions of dollars in economic losses and health crises caused by toxic haze, but also threaten the achievement of national emission-reduction targets under the Forestry and Other Land Use (FOLU) Net Sink 2030 framework (5).

Although national research has historically focused predominantly on mainland areas in western Indonesia, the small islands of eastern Indonesia, particularly Maluku Province and Ambon Island, are increasingly facing alarming levels of fire vulnerability (8). The coastal and hilly areas of Negeri Ureng and Negeri Asilulu, located in Leihitu and West Leihitu Districts on Ambon Island, represent small-island ecosystems characterized by undulating to steep topography and sensitive microclimatic dynamics. In this region, limited land area interacts directly with intense anthropogenic pressures, including traditional agricultural land burning, fuelwood collection, settlement expansion, and the insufficiently regulated management of eucalyptus plantations (8). Given the limited carrying capacity of small-island ecosystems, forest fires in Ureng and Asilulu may cause permanent or irreversible environmental damage, including soil erosion, the degradation of vegetation cover that protects water resources, the loss of endemic species, and disruption of local livelihoods (9).

To minimize ecological and socioeconomic risks, spatial modeling of forest-fire vulnerability based on Geographic Information Systems (GIS) and remote sensing has become an urgent instrument for supporting mitigation and early detection efforts (7,4). Spatial modeling enables the precise delineation of vulnerability zones by integrating historical fire-hotspot data obtained from satellite sensors, such as MODIS and VIIRS/FIRMS, with environmental predictors (10,11). Information on risk zones is highly important for decision-makers in allocating firefighting resources efficiently and designing adaptive spatial-planning strategies (4). Nevertheless, conventional statistical approaches, such as linear regression and bivariate analysis, often have limitations because they are unable to adequately capture complex nonlinear interactions at the local scale within heterogeneous ecosystems (12).

To improve the reliability of spatial modeling, bioclimatic data play a crucial role as primary predictors (13,3). Standardized bioclimatic variables, Bio1 to Bio19 from WorldClim, represent annual and seasonal temperature and precipitation variability, which directly regulate fuel moisture and vegetation dryness. Parameters such as annual mean temperature (Bio1), maximum temperature of the warmest month (Bio5), annual precipitation (Bio12), and precipitation seasonality (Bio15) provide independent information on water stress dynamics and landscape flammability (13,3,14). Before being integrated into the model, multicollinearity testing using Pearson correlation analysis and the Variance Inflation Factor (VIF) is essential for eliminating redundant variables without reducing their ecological transparency and interpretability (11,3).

Methodologically, the Maximum Entropy (MaxEnt) machine-learning algorithm has proven to be one of the most effective methods for modeling the spatial probability of forest-fire vulnerability (4). The main advantage of MaxEnt lies in its ability to process fire-occurrence data in the form of presence-only data without requiring absence data, which are difficult to verify accurately in the field. MaxEnt can evaluate nonlinear relationships between fire-occurrence locations and bioclimatic predictors with high accuracy. Model performance can be evaluated using the Area Under the Curve (AUC) of the Receiver Operating Characteristic (ROC), the True Skill Statistic (TSS), and Jackknife analysis to assess variable contributions.

The research gap underlying this study is the limited availability of high-resolution fire-vulnerability modeling in the small-island ecosystem of Ambon Island, particularly in Ureng and Asilulu, incorporating integrated bioclimatic variables. The novelty of this research lies in identifying bioclimatic response functions and thresholds that are specific to the microscale of a small island. The findings can be utilized by the Regional Disaster Management Agency (BPBD) and local governments as an evidence-based Decision Support System (DSS) for disaster mitigation.

2. Methods

2.1. The study area characteristics

The study area is located within the administrative territories of Negeri Ureng and Negeri Asilulu in Leihitu District, Central Maluku Regency, Maluku Province, Indonesia (Figure 1). Geographically, this area represents a small-island ecosystem landscape with complex topographic variations, ranging from undulating coastal plains to steep hillslopes. The tropical maritime climate of Ambon Island is highly sensitive to interannual climate variability, particularly the El Niño–Southern Oscillation (ENSO), which triggers increases in land-surface temperatures and prolonged dry periods (15). Local vegetation cover is dominated by secondary forests, shrublands, smallholder plantations, and stands of eucalyptus (Eucalyptus/Melaleuca), which are highly flammable because of their essential-oil content when subjected to water stress during the dry season.

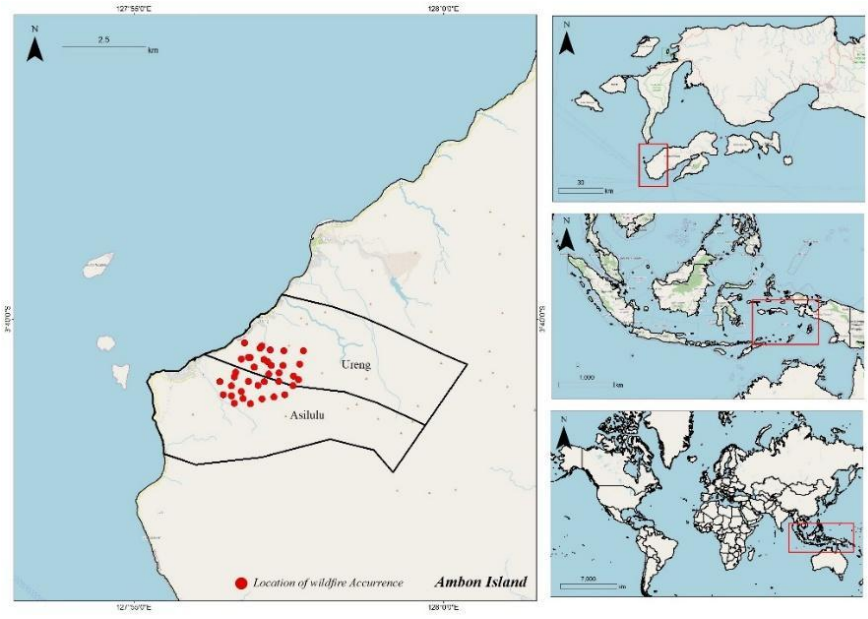


Figure 1. Study Area Location: Negeri Ureng and Negeri Asilulu, Ambon Island, Indonesia

The interaction between highly flammable vegetation types, steep topographic conditions, and intense anthropogenic activities, such as traditional slash-and-burn agricultural practices, fuelwood collection, and the burning of leaf litter around settlements, places Ureng and Asilulu at high risk of forest fires. Given the limited land area and environmental carrying capacity of small-island ecosystems, fire incidents in this region may cause permanent or irreversible ecological impacts, including soil erosion, degradation of vegetation cover that protects water-infiltration areas, loss of endemic flora and fauna, and direct disruption of local livelihoods (2). Therefore, this area is highly suitable as a study site for modeling forest-fire vulnerability based on bioclimatic variables at a microscale.

2.2. Data

2.2.1. Dependent variables: fire occurrence data

The dependent variable used in this study is forest-fire occurrence data represented by hotspot records. A total of 25 historical fire-occurrence points (hotspots, N = 25) within the territories of Negeri Ureng and Negeri Asilulu were extracted from satellite products generated by the Moderate Resolution Imaging Spectroradiometer (MODIS) and the Visible Infrared Imaging Radiometer Suite (VIIRS) sensors through NASA's Fire Information for Resource Management System (FIRMS) platform (3). To ensure data validity and eliminate non-forest thermal anomalies, such as reflections from residential or industrial rooftops, all hotspot points were rigorously filtered by retaining only records with high confidence levels, ranging from 70% to 80% or higher (11).

The 25 verified fire-occurrence points were converted into the WGS 1984 geospatial coordinate system and tested for spatial autocorrelation. Spatial-thinning techniques using buffer thresholds of 500 meters to 1 kilometer were applied to remove duplicate fire-point records occurring repeatedly within the same raster pixel, thereby reducing sampling-cluster bias during the modeling process. The final spatial dataset consisting of 25 filtered fire-presence points, representing presence-only data, was then exported in comma-separated values format (.csv) as the primary dependent input for the MaxEnt model (2).

2.2.2. Predictor variables; Bioclimatic variables

The predictor set must match the variables used to generate the model outputs. The contribution table and Jackknife interpretation identify Precipitation Seasonality (BIO15), whereas the original predictor list identifies Precipitation of the Warmest Quarter (BIO18). For consistency with the reported model outputs, this revised manuscript provisionally lists BIO15 as the fifth predictor alongside BIO1, BIO3, BIO5, and BIO7. The authors must verify this against the actual WorldClim raster files used in MaxEnt before submission. The bioclimatic layers were obtained from WorldClim version 2.1 at 30 arc-seconds (approximately 1 km at the equator) (16). These predictors represent temperature and precipitation conditions relevant to vegetation moisture and fuel drying. Table 1 should be updated to describe BIO15 (Precipitation Seasonality; coefficient of variation of monthly precipitation) if BIO15 was in fact used.

BIO1 and BIO5 describe mean and peak thermal conditions, while BIO3 and BIO7 characterize temperature variability. If confirmed as the fifth input, BIO15 represents the seasonality of monthly precipitation and may help characterize seasonal variation in moisture availability. These variables describe bioclimatic susceptibility; they do not independently represent observed fire incidence or the full set of factors governing fire risk.

Table 1. Summary of Bioclimatic Predictor Variables (BioClim) in MaxEnt Modeling

Bioclimatic Variable	Code	Description & Ecological Relevance to Wildfire Occurrence	Unit	Resolution & Source
Annual Mean Temperature	BIO1	Represents annual mean temperature. Directly influences landscape evapotranspiration, biomass drying rates, and surface fuel temperature elevation.	℃	30 arc-seconds (~1 km²) / WorldClim v2.1
Isothermality	BIO3	The ratio of Mean Diurnal Range to Temperature Annual Range (BIO2/BIO7 × 100). Measures diurnal temperature fluctuation stability relative to annual variability.	%	30 arc-seconds (~1 km²) / WorldClim v2.1
Max Temperature of Warmest Month	BIO5	Maximum temperature during the hottest month. Indicates extreme thermal conditions triggering severe drops in fuel moisture content and lowering ignition thresholds.	℃	30 arc-seconds (~1 km²) / WorldClim v2.1
Temperature Annual Range	BIO7	Difference between max temperature of warmest month and min temperature of coldest month (BIO5 − BIO6). Captures seasonal thermal extremes affecting dry litterfall cycles.	℃	30 arc-seconds (~1 km²) / WorldClim v2.1
Precipitation Seasonality	BIO15	Coefficient of variation of monthly precipitation. Describes the seasonality of precipitation.	mm	30 arc-seconds (~1 km²) / WorldClim v2.1

2.3. Data preparation

Geospatial data preprocessing was conducted using ArcGIS Pro to ensure complete spatial and geometric alignment across all predictor layers (18,4). All bioclimatic raster layers were clipped (*extract by mask*) to the administrative and ecological boundaries of Ureng and Asilulu. Subsequently, spatial coordinates were transformed into the Universal Transverse Mercator system (UTM Zone 52S / WGS 1984), and cell resolution, row counts, and column dimensions were standardized to establish a uniform spatial grid matrix across all layers (19).

Following spatial standardization and handling of no-data values (null values = -9999), the bioclimatic raster layers (BIO1, BIO3, BIO5, BIO7, BIO18) were converted from GeoTIFF to ASCII (.asc) format using ArcGIS Pro (20). ASCII conversion is a mandatory requirement for inputting environmental raster matrices into the MaxEnt software environment

2.4. Selection of predictor variables

Prior to model simulation, the five candidate bioclimatic variables were statistically evaluated for multicollinearity to eliminate variable redundancy that could undermine model stability (11,3). Multicollinearity was assessed by calculating pairwise Pearson correlation coefficients (r) and Variance Inflation Factors (VIF) across all predictor combinations (11,3). Following established MaxEnt modeling standards, predictor pairs exhibiting strong

correlations ($|r| > 0.80$) or VIF values exceeding the threshold (VIF > 10) were excluded (3,21). Statistical testing confirmed that all five selected bioclimatic variables BIO1, BIO3, BIO5, BIO7, and BIO18, satisfied the independence criteria, exhibiting $|r| < 0.80$ and VIF < 10 (3,21,4). Consequently, all five variables were retained, as each provides unique, non-redundant ecological information regarding thermal variations, seasonal fluctuations, and landscape moisture stress in Ureng and Asilulu without introducing collinearity bias.

2.5. Modeling the likelihood of fire occurrence

Forest fire susceptibility modeling was executed using MaxEnt software (version 3.4.4), a machine learning algorithm rooted in the maximum entropy principle (22,23). MaxEnt estimates the spatial probability distribution of fire occurrences by evaluating bioclimatic conditions at known fire points (*presence-only data*) against a random sample of background points representing environmental conditions across the entire study area (24,18). Mathematically, MaxEnt applies Shannon's information theory to find the probability distribution *p(x)* with maximum entropy (most uniform) subject to constraints imposed by observed environmental feature expectations (24,18). Information entropy *H(p)* is defined in Equation 1 (24):

$$H\ (p) = -\sum_{x \in X} \quad p\ (x)\ ln\ p(x) \tag{1}$$

where $p(x)$ represents the probability density of fire occurrence at spatial pixel location x within the landscape domain X (24). To incorporate predictor variables, MaxEnt constructs a Gibbs distribution $q\lambda(x)$ under the constraint that the expected value of each environmental feature $f_j(x)$ under $q\lambda$ matches its empirical average observed at presence locations (25). The probability distribution formula is expressed in Equation 2, (18,26):

$$q\lambda(x) = \frac{1}{Z_\lambda}\ exp\ \left(\sum_{j=1}^{m} \quad \lambda_j f_j(x)\right) \tag{2}$$

Where $f_j(x)$ denotes feature functions (e.g., linear, quadratic, hinge, or product) derived from the five bioclimatic predictors (BIO1, BIO3, BIO5, BIO7, BIO18), (25,14), λ_j represents feature weight coefficients optimized through regularization to prevent overfitting (27,18), and Z_j is a normalizing partition function calculated via Equation 3:

$$Z_\lambda = \sum_{x \in X} \quad exp\ \left(\sum_{j=1}^{m} \quad \lambda_j f_j(x)\right) \tag{3}$$

The raw suitability density $q\lambda\ (x)$ is subsequently transformed into continuous probability values ranging from 0 to 1 using the complementary log-log (cloglog) transformation (15), as formulated in Equation (4):

$$P_{clonglog}\ (x) = 1 - exp\ \left(-e^{\eta\ (x)}\right) \tag{4}$$

Where $\eta\ (x) = \sum_{j=1}^{m} \quad \lambda_j f_j(x) - ln\ Z_\lambda + exp\ H_{Prior}$ represents the exponent calculated from weighted environmental features (Elith et al., 2011; Göltaş et al., 2024).

Given the specific fire sample size in the study area (N = 25 hotspots), a 10-fold cross-validation or random split scheme (70% training set / 18 points and 30% testing set / 7 points) was implemented to optimize evaluation power without over-parameterizing the model (11,3). Simulations were executed with 10–20 bootstrap replicates using a regularization multiplier of 1 to manage model complexity (11,3).

Predictive performance and model accuracy were quantitatively evaluated using Receiver Operating Characteristic (ROC) curves by calculating the Area Under the Curve (AUC) and the True Skill Statistic (TSS) (3). The area under the ROC curve is defined mathematically in Equation 5:

$$AUC = \int_0^1 TPR\ (FPR)\, d\,(FPR) \quad (5)$$

Where $TPR = \frac{TP}{TP+FN}$ represents the True Positive Rate (Sensitivity) and $FPR = \frac{TP}{FP+TN}$ represents the False Positive Rate (1 - Specificity) (27). Models achieving AUC values between 0.80 and 0.90 are classified as having good-to-excellent accuracy (Chepashev et al., 2025; Paudel et al., 2024). Jackknife testing was conducted to evaluate the percentage contribution and permutation importance of each individual BioClim variable (11,3). Finally, continuous probability output rasters were imported into ArcGIS Pro and reclassified into five fire vulnerability zones (Very Low, Low, Moderate, High, and Very High) using equal interval or natural breaks methods to generate actionable risk maps for emergency management and spatial planning (11,3).

3. Results and Discussion

3.1. Results

3.1.1. Analysis of Maxent model results

The evaluation of omission rates indicates that the omission rate on test samples closely aligns with the predicted omission rate. This strong congruence between the test omission line and the theoretical prediction line confirms the stability and robustness of the MaxEnt model, demonstrating that the model does not suffer from overfitting and possesses high generalization capacity when evaluated against independent test data (27,22). Furthermore, this close alignment confirms that the applied cumulative thresholds consistently minimize omission errors across observed fire occurrence locations.

Based on the Area Under the Curve (AUC) value of 0.94 (Figure 2), the predictive performance of the MaxEnt model is categorized as achieving an excellent discrimination capability. An AUC value of 0.94 substantially exceeds the 0.50 threshold of a random prediction model, indicating that the MaxEnt algorithm performs significantly better in predicting fire occurrences and differentiating fire-vulnerable areas from background points across the landscape (28,23,4). This high spatial separability underscores that the selected combination of environmental predictors effectively captures the primary ecological drivers governing forest fire susceptibility in the study area.

3.1.2. Analysis of variable contributions

The relative contribution analysis of environmental variables in the MaxEnt model indicates that precipitation seasonality and thermal regimes serve as the primary drivers

governing forest fire occurrence across the study area. Precipitation seasonality (Bio15) dominated the model, accounting for a percentage contribution of 54.6% and a permutation importance of 55.4%. This substantial contribution underscores that inter-seasonal rainfall variability heavily regulates fuel moisture dynamics and accelerates vegetation flammability thresholds during dry periods. The second most influential predictor was Annual mean temperature (Bio1), exhibiting a percentage contribution of 24.7% and a permutation importance of 27.0%. High Bio1 values reflect elevated mean atmospheric temperatures that directly increase landscape evapotranspiration rates and accelerate surface biomass drying. Cumulatively, Bio15 and Bio1 account for more than 79% of the model's predictive power, demonstrating that seasonal water stress and cumulative thermal exposure are the dominant triggers of wildfire susceptibility across the landscape.

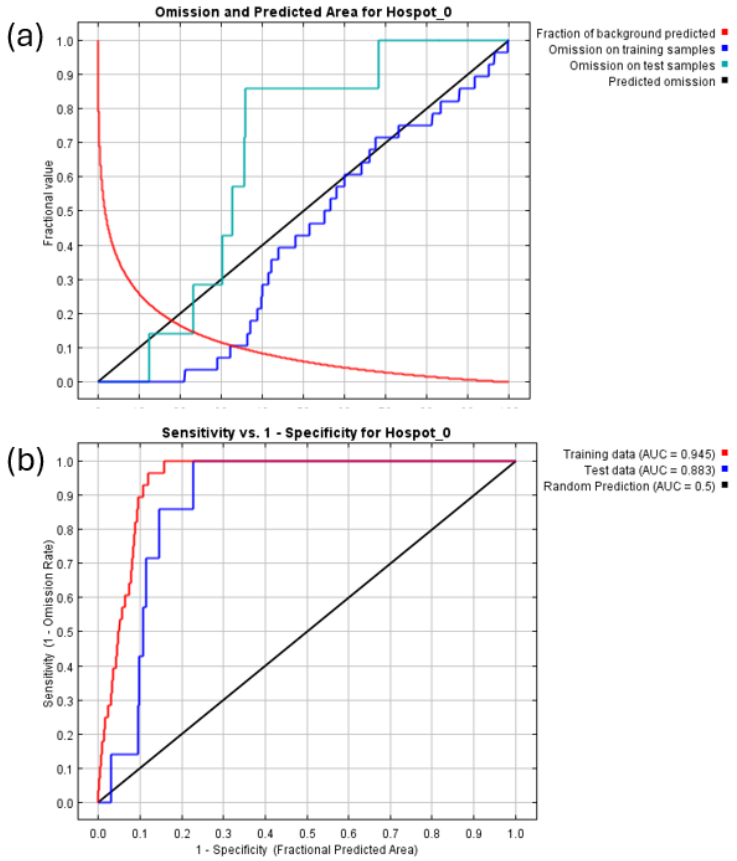


Figure 2. (a) Omission analysis of the MaxEnt model for both the training and testing datasets. (b) Receiver operating characteristic (ROC) curves for the training and testing datasets, with predictive performance evaluated using the area under the curve (AUC).

Meanwhile, Isothermality (Bio3) exerted a moderate influence, yielding a percentage contribution of 12.8% and a permutation importance of 12.1%, which highlights the role of diurnal temperature stability relative to annual fluctuations in modulating microclimatic conditions. The remaining two predictors, Precipitation of warmest quarter (Bio18) and Temperature annual range (Bio7), accounted for lower percentage contributions of 5.7% and 2.1%, respectively. Although Bio7 exhibited a relatively minor training contribution, its permutation importance of 5.5% (compared to 0% for Bio18) indicates that Bio7 provides unique, independent ecological information that substantially impacts model accuracy when

its values are permuted. Overall, the synthesis of training contribution rates and permutation importance confirms that wildfire vulnerability in the study area is driven by complex, non-linear interactions between seasonal rainfall unpredictability and extreme thermal conditions.

Table 2. Relative contribution of each environmental variable to the MaxEnt model predicting fire occurrence.

No	Predictor variables	Percentage contribution (%)	Permutation importance
1	Precipitation seasonality (Bio15)	54,6	55,4
2	Annual mean temperature (Bio1)	24,7	27
3	Isothermality (Bio3)	12,8	12,1
4	Precipitation of warmest quarter (Bio18)	5,7	0
5	Temperature annual range (Bio7)	2,1	5,5

3.1.3. Jackknife analysis of predictor importance

Based on Figure 3, the results of the MaxEnt Jackknife test demonstrate distinct variations in the relative contributions of environmental predictors to the regularized training gain. The baseline training gain achieved when incorporating all environmental variables (with all variables) reached approximately 1.23, providing a reference benchmark for evaluating individual variable significance. When assessing model performance upon variable exclusion (without variable), Precipitation Seasonality (BIO15) yielded the lowest regularized training gain at approximately 1.14, whereas BIO1, BIO18, BIO3, and BIO7 maintained higher gains ranging between 1.20 and 1.23. This pronounced drop in training gain when BIO15 is omitted confirms that BIO15 possesses the most substantial unique information content essential for explaining fire hotspot occurrences, making it the most influential predictor under the Jackknife evaluation framework (23,16,4).

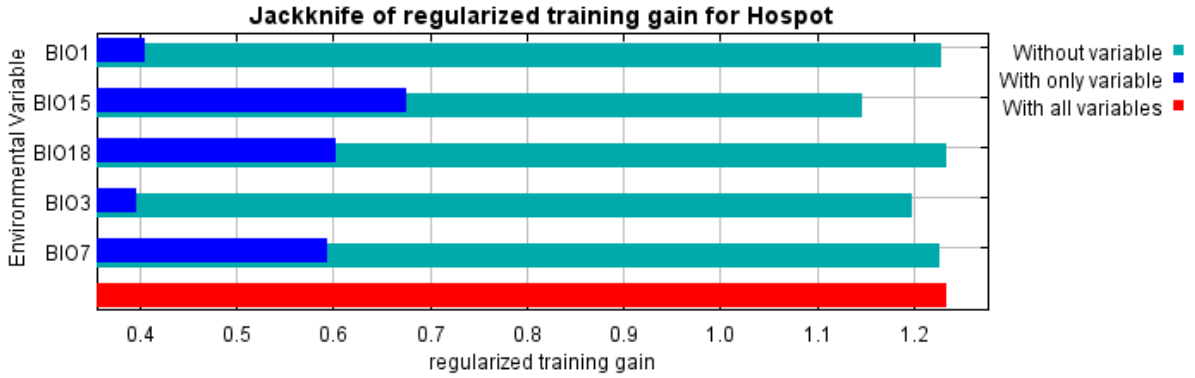


Figure. 3. The results of the analysis variable importance using the jackknife test.

Similarly, when evaluating single-variable predictive performance in isolation (with only variable), BIO15 achieved the highest individual regularized training gain at approximately 0.68, followed by BIO18 (~0.60), BIO7 (~0.59), BIO1 (~0.40), and BIO3 (~0.39). This hierarchy indicates that BIO15 exhibits the strongest standalone predictive capability among all evaluated environmental drivers (16,4). Within the context of Analysis of Spatial Geometric Distortion and Boundary Shift, the pronounced dominance of BIO15 indicates that spatial fluctuations in seasonal rainfall heavily govern the spatial geometry and boundary

distribution of predicted fire hotspots (14,23). Consequently, perturbations or instability in BIO15 values exert a disproportionately greater influence on spatial boundary shifts in high-vulnerability risk zones across the small-island landscape of Ureng and Asilulu compared to other environmental variables .

3.1.4. Spatial distribution of fire risk

The classified map covers a reported area of 281.7909 km² represented by 313,101 raster cells. These figures imply a mean cell area of approximately 900 m², equivalent to a 30 m grid, which differs from the approximately 1 km native resolution of the WorldClim predictors. The manuscript must document the resampling method, output cell size, projection, and pixel-counting procedure; a finer output grid should not be presented as finer climatic information. The Very Low class covers 187.6041 km² (66.58%), and the Low class covers 42.7923 km² (15.19%), giving a combined 230.3964 km² (81.77%). The Moderate Risk area is not reported in the supplied results and cannot be derived reliably from the current summary alone. It must be calculated from the final classified raster and added to the area table/text so that all five classes sum to the total mapped area and 100%, allowing for rounding (11,4).

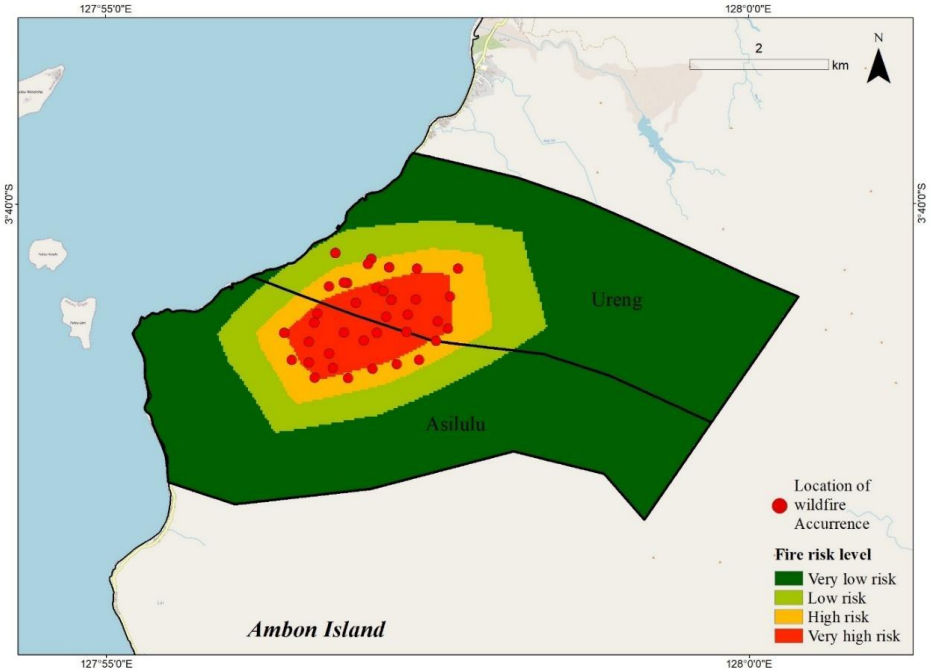


Figure 4. A map showing the predicted fire occurrence risk level for each [area/pixel] in Ureng and Asilulu Villages.

Conversely, areas exposed to substantial wildfire threats are categorized into two primary risk tiers: the High Risk zone encompassing 25.3206 km² (8.99%) and the Very High Risk zone covering 26.0739 km² (9.25%). Combined, the cumulative high-threat area (*High* and *Very High Risk*) encompasses 51.3945 km² or 18.24% of the total landscape (Figure 4). Although representing less than one-fifth of the total area, the concentration of high-vulnerability zones spanning 51.39 km² warrants stringent disaster management prioritization. These identified high-risk zones provide crucial spatial intelligence for the Regional Disaster Management Agency (BPBD) and local forestry officers to strategically allocate firefighting assets, establish

early warning systems, and regulate human-induced ignition activities during extreme drought periods (25,6,4).

3.2. Discussion

The reported AUC of 0.94 indicates strong discrimination between test presence locations and background conditions under the model's evaluation design. However, the small sample of 25 presence points and the unresolved description of the validation configuration mean that claims of stability, absence of overfitting, and generalization should be made cautiously. The map is best interpreted as a preliminary model of bioclimatic susceptibility rather than a validated prediction of actual fire occurrence. Its reliability also depends on the spatial distribution and quality of hotspot records, the selection of background points, and the verified predictor set.

The dominance of Precipitation Seasonality (BIO15) as the most influential variable indicates that seasonal precipitation variability is the primary ecological factor controlling fire vulnerability in the study area. BIO15 contributed 54.6% to the model, with a permutation importance of 55.4%, while Annual Mean Temperature (BIO1) was the second most influential factor, contributing 24.7% with a permutation importance of 27.0%. Collectively, these two variables accounted for more than 79% of the model contribution, indicating that seasonal hydrological stress combined with thermal conditions represents the major control of fire vulnerability. The Jackknife analysis further supports this finding, as removing BIO15 resulted in the largest decline in training gain, from approximately 1.23 to 1.14. BIO15 also produced the highest training gain when evaluated individually, reaching approximately 0.68. These results indicate that seasonal variations in precipitation play an important role in controlling vegetation moisture and surface fuel availability. When dry periods become more pronounced, declining vegetation moisture can increase fuel flammability and consequently enhance the likelihood and potential spread of forest fires.

The mapped Very Low and Low classes cover 230.3964 km² (81.77%), while the High and Very High classes cover 51.3945 km² (18.24%); the Moderate class area must be added after recalculation from the classified raster. These figures should be interpreted only after confirming that the five class areas reconcile with the total mapped area. Bioclimatic susceptibility is one component of fire risk, which also depends on ignition sources, land cover, fuel continuity, land-use practices, and human access. Consequently, the map should guide screening and field verification rather than be used alone to allocate response resources or declare locations safe. In Ureng and Asilulu, locally actionable measures include community fire-prevention outreach, monitoring during seasonally dry periods, safer agricultural-burning practices, rapid reporting of smoke or hotspots, and coordination with village authorities and fire services. On these small islands, preventing vegetation loss is especially important for protecting biodiversity, limiting erosion on steep slopes, maintaining infiltration and watershed functions, and supporting climate adaptation and local livelihoods.

Conclusions

This study demonstrates that the Maximum Entropy (MaxEnt) approach can effectively model and map forest fire vulnerability in Negeri Ureng and Negeri Asilulu, Ambon Island, with excellent predictive performance, as indicated by an AUC value of 0.94 and close agreement between the test omission rate and the predicted omission rate. Variable contribution analysis showed that Precipitation Seasonality (BIO15) was the most dominant

environmental factor, with a contribution of 54.6% and a permutation importance of 55.4%, followed by Annual Mean Temperature (BIO1), with a contribution of 24.7% and a permutation importance of 27.0%. The dominance of BIO15 was further supported by the Jackknife analysis, which showed the largest decline in training gain when this variable was excluded from the model. Spatially, most of the study area, covering 230.3964 km² or 81.77%, was classified as Very Low and Low Risk. However, areas classified as High and Very High Risk still covered 51.3945 km² or 18.24% of the total study area. These findings indicate that forest fire vulnerability has a heterogeneous spatial distribution and is primarily associated with seasonal precipitation variability and temperature conditions. Therefore, the resulting vulnerability map can serve as a basis for prioritizing fire monitoring, developing early warning systems, and implementing fire mitigation strategies, particularly in areas with High and Very High Risk during periods of increasing seasonal drought stress.

Funding

This research received no external funding.

Acknowledgments

We extend our gratitude to all parties who have assisted in this research.

Conflicts of Interest

The authors declare no conflict of interest.

References

1. Chervier C, Atmadja SS, Nofyanza S, Nur C, Nurfatriani F, Kristiningrum R, et al. Impact of Indonesia ' s Forest Management Units on the reduction of forest loss and forest fires in Sulawesi. Ecol Econ. 2025;227(April 2024):108418.
2. Goltas M, Sinclair AL, Lb L, Cochrane MA, Saharjo BH, Thomas A, et al. Ecological Risk Assessment and Management of Forest Fires in Tamil Nadu, India: A MaxEnt Model-Based Approach for Strategic Resource Allocation and Fire Mitigation. Risk Anal. 2025 Nov 4;45(11):3604–25.
3. Mupfiga U, Mutanga O, Dube T. Assessing drivers of vegetation fire occurrence in Zimbabwe - Insights from Maxent modelling and historical data analysis. Remote Sens Appl Soc Environ. 2025;37:101404.
4. Paudel G, Pandey K, Lamsal P, Bhattarai A, Bhattarai A, Tripathi S. Geospatial forest fire risk assessment and zoning by integrating MaxEnt in Gorkha District , Nepal. Heliyon. 2024;10(11):e31305.
5. Purnomo H, Puspitaloka D, Okarda B, Andrianto A, Jalil A, Prasetyo P, et al. Community-based fire prevention and peatland restoration in Indonesia : A participatory action research approach. Environ Dev. 2024;50(October 2022):100971.
6. Karurung WS, Lee K, Lee W. Assessment of forest fire vulnerability prediction in Indonesia: Seasonal variability analysis using machine learning techniques. Int J Appl Earth Obs Geoinf. 2025;138:104435.
7. Agustiyara A, Koren G, Székely B. Comparative assessment of forest fire susceptibility and risk mapping in Riau Peatlands, Sumatra using remote sensing. Remote Sens Appl Soc Environ. 2026;42:102066.
8. Abdul Muin & HR. Pemetaan Kerentanan Kebakaran Hutan di Pulau Buru, Provinsi

Maluku Berdasarkan Fire Hotspot. INSOLOGI J Sains Dan Teknol. 2023;2(4):675–83.
9. Herdian, A., Boreel, A., & Loppies R. Tingkat kerawanan kebakaran hutan dan lahan menggunakan sistem informasi geografis (SIG) di Kota Ambon (studi kasus di jazirah leitimur selatan). J HUTAN PULAU-PULAU KECIL. 2021;5(1):1-13.
10. Suhardono S, Fitria L, Suryawan IWK, Septiariva IY, Mulyana R, Sari MM, et al. Human activities and forest fires in Indonesia: An analysis of the Bromo incident and implications for conservation tourism. Trees, For People. 2024;15:100509.
11. Chepashev D, Nurakynov S, Sharma D, Sydyk N, Kabdulova G. Mapping fire hazard potential in Kazakhstan: a machine learning and remote sensing perspective. Int J Wildl Fire. 2025 Aug 20;34(9):WF24232.
12. Castro M, Ritonga R, Masuda Y, Asyhari A, Novita N, Gangga A, et al. Effective restoration can avoid peatland fires: Large scale counterfactual assessment in Kalimantan, Indonesia. iScience. 2026;29(6):116041.
13. Goltas M. Predicting forest fire probability under current conditions and future climate change scenarios in Türkiye. For Ecosyst. 2026;17:1–13.
14. Jaouani M, Boubekraoui H, Ghallab A. Spatio-temporal analysis and MaxEnt modeling of wildfires in the Tangier-Tetouan-Al Hoceima region (northern Morocco). Kuwait J Sci. 2027;54(1):100691.
15. Usmadi D. Maximum entropy application in predicting the vulnerability of land and forest fires in South Sumatra Province, Indonesia. IOP Conf Ser Earth Environ Sci. 2023 May;1183(1):12105.
16. Mupfiga U, Mutanga O, Dube T. Remote Sensing Applications : Society and Environment Assessing drivers of vegetation fire occurrence in Zimbabwe - Insights from Maxent modelling and historical data analysis. Remote Sens Appl Soc Environ. 2025;37:101404.
17. Apriliyanti ID, Nugraha DB. Burning coal in a cleaner way: Institutional fragmentation, power dynamics, and business influence in Indonesia's biomass co-firing imaginaries. Energy Res Soc Sci. 2025;121:103949.
18. Lorenț A, Petrila M, Apostol B, Capalb F, Chivulescu Şerban, Şamşodan C, et al. Assessing and Mapping Forest Fire Vulnerability in Romania Using Maximum Entropy and eXtreme Gradient Boosting. Vol. 16, Forests. 2025. p. 1156.
19. Suryawan IWK, Suhardono S, Sofiyah ES, Rahman A, Ulhasanah N, Sari MM, et al. Integrated climate governance framework for forest fire management: A hypothetical application in Indonesia. Trees, For People. 2026;24:101145.
20. Butar Butar MB, Nasution S, Parinduri AH, Zaen M. Traceability-based environmental burden indicators for Indonesia's pulp sector: Corporate-group evidence from forest-risk supply chains. Environ Sustain Indic. 2026;32:101526.
21. Fadiilah D, Dye A. Early retirement of coal-fired power plants in Indonesia : A comprehensive analysis of emissions (from Sentinel 5p and HYSPLIT) and population impact. Total Environ Adv. 2026;17(x):200145.
22. Elith J, Phillips SJ, Hastie T, Dudík M, Chee YE, Yates CJ. A statistical explanation of MaxEnt for ecologists. Divers Distrib. 2011 Jan;17(1):43–57.
23. Meraj G, Hashimoto S, Dasgupta R, Mitra BK. Ecological Risk Assessment and Management of Forest Fires in Tamil Nadu, India: A MaxEnt Model-Based Approach for Strategic Resource Allocation and Fire Mitigation. Risk Anal. 2025;45(11):3604–25.
24. Choi J, Chae H. Assessing Wildfire Risk in South Korea Under Climate Change Using the Maximum Entropy Model and Shared Socioeconomic Pathway Scenarios. 2025;

25. Goltas M. Predicting forest fire probability under current conditions and future climate change scenarios in Türkiye. For Ecosyst. 2026;17(July):100525.
26. Phillips SJ, Anderson RP, Dudík M, Schapire RE, Blair ME. Opening the black box: an open-source release of Maxent. Ecography (Cop). 2017 Jul 9;40(7):887–93.
27. A DC, A SN. Mapping fire hazard potential in Kazakhstan : a machine learning and. Int J Wildl Fire. 2024;1–20.
28. Xu H, Jiang C, Li X, Fan H, Wang J, Li J. Optimized MaxEnt modeling reveals major decline and shift of giant panda habitat under CMIP6 ensemble projections. Ecol Indic. 2025;179:114150.

CC BY-SA 4.0 (Attribution-ShareAlike 4.0 International).
This license allows users to share and adapt an article, even commercially, as long as appropriate credit is given and the distribution of derivative works is under the same license as the original. That is, this license lets others copy, distribute, modify and reproduce the Article, provided the original source and Authors are credited under the same license as the original.